

APPLIED SCIENCE DIVISION  
Litton Systems, Inc.  
2003 East Hennepin Avenue  
Minneapolis, Minnesota 55413

INVESTIGATION OF SPUTTERING EFFECTS ON  
THE MOON'S SURFACE

Twelfth Quarterly Status Report  
Contract NASw-751

Covering Period 25 January 1966 to 24 April 1966

Submitted to:

National Aeronautics and Space Administration Headquarters  
Office of Lunar and Planetary Programs, Code SL  
Washington, D.C. 20546

Prepared by:

G. K. Wehner  
C. E. KenKnight  
D. L. Rosenberg

Report No. 2986  
Date: 25 May 1966  
Project: 89308

Submitted by:

*G. K. Wehner*  
G. K. Wehner, Director  
Surface Physics Laboratory

## TABLE OF CONTENTS

<u>Section</u>	<u>Title</u>	<u>Page</u>
	LIST OF ILLUSTRATIONS	iii
	ABSTRACT	1
I.	INTRODUCTION	2
II.	CRUST BUILDUP ON A POWDERED SURFACE BY ION BOMBARDMENT	3
III.	THE EFFECT OF SPUTTERING ON POROUS MEDIA	4
IV.	MODIFICATION OF OPTICAL PROPERTIES OF THE LUNAR SURFACE BY SOLAR-WIND BOMBARDMENT	5
	A. INTRODUCTION	5
	B. APPARATUS	9
	1. Sputtering Equipment	9
	2. Reflectometer	14
	3. Criticisms of Equipment and Procedure	17
	C. RESULTS	21
	1. Composition Dependence	21
	2. Influence of Surface Structure	29
	3. Influence of Particle Size	46
	D. CONCLUSIONS	47
	REFERENCES	50

# LIST OF ILLUSTRATIONS

<u>Figure</u>	<u>Caption</u>	<u>Page</u>
1	Schematic of plasma bombardment system.	11
2	Reflectometer used in photometric and polarimetric measurements.	15
3	Dependence of albedo upon photon frequency for rock powders and for the mean moon (Harris, 1961).	24
4	Albedo-color diagram for samples of finely divided rock and for lunar features (Gehrels <u>et al.</u> , 1964). Line segments connect measurements on a single sample surface; changes are due to ion bombardment.	26
5	Photometric functions $F(\alpha)$ in green light of: 1) Mare Tranquillitatis, latitude $39^{\circ}3'$ , according to Gehrels, <u>et al.</u> (1964), 2) Sifted $10\text{-}20\mu$ tholeiitic basalt powder, $A_n = 0.107$ , 3) Same powder compacted by shaking, $A_n = 0.110$ . Curves (a) are for $\epsilon = 0^{\circ}$ , (b) for $\epsilon = 50^{\circ}$ , (c) for $\epsilon = 50^{\circ}$ with light source between detector and the surface tangent plane. Curves (a), (b), and (c) are not arbitrarily placed but are related by limb-darkening effects. The circled points in (1) correspond to curves (b); the others correspond to curves (c).	32
6	Photometric function $F(\alpha)$ at $\epsilon = 0^{\circ}$ for sifted $0\text{-}20\mu$ greenstone powder. The function depends markedly on the wavelength of the scattered light. (a) Red light, (b) Green light, (c) Ultraviolet light. 1) Unspattered, 2) $10^4$ equivalent year, 3) $10^5$ equivalent year.	38
7	Decrease in the photometric function $F(\alpha)$ from $ \alpha  = 5^{\circ}$ to $20^{\circ}$ for green light for powder samples of various particle sizes and composition, and for the moon. Measurements on a surface whose albedo was decreased by sputtering are connected by line segments.	41
8	Measurements of the depolarizing ratio $R$ for various powder surfaces for which the albedo in green light is also known. Lunar values are due to Dollfus (1955). Line segments indicate surfaces darkened by sputtering. Vectors indicate the corrections discussed in the text that are necessary to put the laboratory and lunar measurements on the same basis.	44

INVESTIGATION OF SPUTTERING EFFECTS ON  
THE MOON'S SURFACE

Twelfth Quarterly Status Report  
Contract NASw-751

ABSTRACT

Attempts to build up thick crusts of powders which are ion bombarded during deposition and the study of changes in the permeability of solid rock samples due to ion bombardment were continued. A summary of the optical properties of the moon in comparison to those of ion bombarded powder samples is given in preparation for publishing the work of the last three years. Trends in sample color due to composition differences are presented. Though the color of lunar features should permit identification of composition differences after taking decoloration effects of the solar wind into account, positive identification is not now possible. A number of properties of the lunar photometric function plus the polarization of earthshine are shown to be incapable of proving whether the lunar surface is underdense or compacted. The photometric function reveals that the lunar surface has a rough macrostructure, the form of which may correspond in general to that seen in the photographs of Luna 9. The earlier conclusion that the polarization of moonlight is in good agreement with that of light scattered from powders whose particles are mostly less than 0.1 mm in size is not modified by the latest consideration of composition, density, and roughness of the lunar surface layer.

## I. INTRODUCTION

The Eleventh Quarterly Status Report included work from a portion of the twelfth quarter and therefore our section on new experimental work is shorter than usual. Certain experimental phases of the photometric work were completed and our main effort in this quarter was directed towards preparing the material of the last three years for a publication in the Journal of Geophysical Research.

An interesting and helpful visit was made to the Minneapolis Research Center of the United States Bureau of Mines at the end of April. This group heads a research project funded by NASA titled "Multidisciplinary Research Leading to the Utilization of Extraterrestrial Resources".

Charles KenKnight attended the 12 May meeting of the Subgroup on Mining and Processing of the Working Group on Extraterrestrial Resources. The meeting was also attended by our contract monitor, Robert P. Bryson, and a helpful discussion concerning our present and future work was held.

## II. CRUST BUILDUP ON A POWDERED SURFACE BY ION BOMBARDMENT

The properties of a thick crust of powder uniformly ion bombarded throughout would be of great interest. Previously we had built up a 7 mm thick crust of mercury ion bombarded  $\text{Cu}_2\text{O}$  particles. Every 6 min an automated shaker device would deposit a small amount of  $\text{Cu}_2\text{O}$  onto a tantalum plate while the plate was being continuously bombarded by 250 eV mercury ions. In approximately 30 hr a 7 mm crust was built up. The crust was fragile but the cementation was adequate to allow inversion of the substrate without loss of powder. A control experiment with exposure of the powder to plasma only was run but the powder fell off when the substrate was tilted approximately  $60^\circ$ .

Recently an electromagnetic shaker device, as used in flash evaporation sources, was obtained from Balzers (Liechtenstein) capable of delivering a small uniform stream of powder in a vacuum environment. In our plasma environment we experienced difficulties with outgassing of the driving mechanism which is not built to withstand higher temperatures ( $>150^\circ\text{C}$ ). We have now completed the construction of a modified version of this device with the driving mechanism outside the vacuum system. We hope to soon deposit uniformly thick sputtered crusts suitable for optical photometry and polarization measurements and at least qualitative strength measurements.

### III. THE EFFECT OF SPUTTERING OF POROUS MEDIA

The reduction of the permeability of a porous surface layer by heavy ion bombardment was described in the Tenth Quarterly Status Report. Fritted glass and porous nickel filters were partially "sealed up" by argon ion bombardment. Hydrogen ion bombardment of these filters either had no measurable effect or tended to "open up" the surface. An attempt to repeat these experiments on smooth solid rock surfaces was not successful due to our inability to measure the low permeabilities involved. The filter porosity measuring apparatus, utilizing a wet test meter and absolute pressure meter, could not measure the low air flow rates. A CEC helium leak detector was tried but in this case the leak rates involved were too high. We became aware of a possible solution to the permeability measuring problem while recently visiting the U. S. Bureau of Mines, Twin Cities Mining Research Center. They have offered to measure the permeability of our rock samples with their standard measuring apparatus which employs fluids at high pressures. Our plasma bombardment vacuum system is presently being used for water formation studies but we hope to resume bombardment of solid rock surfaces in the near future.

#### IV. MODIFICATION OF OPTICAL PROPERTIES OF THE LUNAR SURFACE BY SOLAR-WIND BOMBARDMENT

##### A. INTRODUCTION

The intensity and polarization of light scattered from the moon can reveal average microscopic properties of the scattering surface not resolvable even in the photographs of Luna 9. It is well known that the absence of limb-darkening for the full moon and the absence of a bright (specular) spot along the intensity equator of the moon at other phases requires a rough lunar surface (e.g., Minnaert, 1961). The brightness of the whole moon or of its features decreases rapidly away from full moon in a manner implying a roughness so great that it is comparable to that of the loosely ramified lichen Cladonia rangiferina (Van Diggelen, 1958; Hapke and Van Horn, 1963). The scale of this roughness is not established by these considerations of the intensity of moonlight, but the low value of the polarization of the light led early workers to conclude that the scattering was principally from a powder (Wright, 1927; Lyot, 1929; see also F. E. Wright et al., 1963, and Dollfus, 1961). We assume that this conclusion is correct and confine our attention to the scattering properties of powder surfaces. In fact, we will show that the polarization demands scattering from particles smaller than about 0.1 mm. It is true that the polarization of light scattered from randomly oriented rock surfaces at the phase of quarter moon would be considerably less than that from a smooth rock surface oriented to give specular reflection. But random surface orientation is not sufficient to explain the low polarization of moonlight; small particles are required.



Lyot (1929) asserted that a certain volcanic ash exhibited qualitative agreement with the moon with regard to color, strong scatter of light back toward the light source, and polarization of the scattered light. But quantitative agreement was not established. Since that time a great wealth of precision lunar measurements, both photometric and polarimetric and for various wavelengths, have been accumulated which must be considered. It is our purpose to find quantitative agreement with the optical properties of the moon.

It was suggested by Wehner (1961) that the solar wind might cause important sputtering effects on the moon's surface. In particular, he expected that in sputtering atoms from a rough surface, constituents like oxygen might be preferentially lost while metals might be retained. This would be partly due to velocity-filtering of the sputtered atoms in the lunar gravitational field and partly due to the lower probability that an oxygen atom will be adsorbed on the first obstruction that it encounters. As a consequence, sputtered compounds like silicate rocks could become more absorbent to light and be reduced in albedo. In subsequent experiments, where the solar wind was simulated by laboratory plasmas, darkening effects were observed which were quite marked in times corresponding to geologically short times on the order of  $10^4$  yr (Wehner et al., 1963a, b; Rosenberg and Wehner, 1964). Spurious darkening of an ion bombarded surface due to deposition of contaminants from the vacuum system is possible, but Hapke (1965a, b) has found comparable darkening rates. Each group found that pure MgO powder darkened very little after the equivalent of  $10^5$  yr on the moon. Therefore

spurious darkening due to deposition seems improbable, but further experiments are needed to establish the darkening rates more carefully. In particular, some account must be taken of the possible selection effect of the lunar escape velocity  $v_c$  because sputtered atoms from a number of metals have velocities comparable to  $v_c$  (Wehner et al., 1963a; Stuart and Wehner, to be published). But there are no data on velocities of atoms sputtered from compounds by hydrogen and helium ions or, indeed, any other ions. The position adopted here is that the darkening rate due to the solar wind striking the lunar surface may be incorrect by an unknown scale factor but that the darkening rate is non-zero.

The variables which affect the optical properties of a powder surface are powder composition, particle size, and surface structure. In addition, we introduce the variable of ion dose. The measurements that we report are color (brightness at a small phase angle relative to a reference MgO surface normal to the incident light), shape of the photometric function at various angles of emergence from the sample surface for light (or several wavelengths) scattered in a plane including the normal to the sample, and values of the polarization of (mostly) green light at those angles of emergence. The quantities to be interrelated are indicated in Table 1.

TABLE 1. Measured Quantities and Variables to be Considered  
in Comparing Various Powder Surfaces to the Moon

Measured		Variables
Albedo and color	$b(\alpha = 2.5^\circ; \lambda)$	Composition
Relative intensities	$b(i, \epsilon; \lambda)/b(2.5^\circ)$	Particle Size
Polarization	$P(\alpha, \epsilon; \lambda)$	Surface Structure
		Sputtering Dose

Fortunately, some economies can be realized in the number of relationships that must be considered. For example, changes in composition affect principally the sample color, albedo, and rate of change of albedo with ion dose, but affects relative intensities and polarization only through opacity of the particles. We will compare the measured quantities to lunar data in an effort to limit the possible range of values of the independent variables that could be represented on the moon. However, no serious effort will be made to establish which composition best fits the moon because of the uncertainties associated with possible spurious darkening in the laboratory simulation of the solar wind and possible differential effects in the gravitational field of the moon. Instead, trends due to composition differences will be pointed out.

## B. APPARATUS

### 1. Sputtering Equipment

In order to simulate solar-wind bombardment times of  $10^3$  to  $10^5$  yr, one needs ion doses of 1 to  $100 \text{ C/cm}^2$ . Fairly intense ion current densities (of the order of a few milliamperere per square centimeter) must be used in order to keep bombardment times within reason. Use of an ion beam is feasible and permits controlled variation of the angle of incidence, the energy, and identity of the ions. Care must be taken, though, to be certain that beam ions or fast neutral atoms arising from charge exchange of beam ions are not sputtering metal from the accelerating electrodes onto the sample. Work with mass-separated ion beams extracted from a duoplasmatron source is presently in progress. In the work discussed here we chose to draw ions out of a discharge plasma. This method is much simpler and sufficient for obtaining a survey of the main effects.

In drawing ions from a plasma, one must maintain an electric field to accelerate the ions toward the sample surface. For insulating samples a charge accumulates at the surface until the electric field vanishes. This difficulty is overcome by employing a radio frequency method in which a high frequency voltage (2.5 Mc/sec) is applied to a metal electrode behind the insulator material to be bombarded and to a reference electrode also immersed in the plasma (Anderson et al., 1962). Since the mobility of electrons is much greater than that of the ions, a rectifying action occurs at each of the electrodes. The sample surface is driven negative with respect to the plasma during most of a cycle and is then bombarded by a nearly constant current of ions whose energies vary from thermal to a maximum midway

in the ion bombarding cycle. In our case the maximum is about 800 ev. In the small remainder of the cycle, neutralizing low energy electrons are drawn to the sample surface. At the much larger reference electrode (2 sides of 45 cm<sup>2</sup> Ta sheet, about 50 times the target area), the same process develops voltages too small for sputtering. Sputtering of Ta (for Ne, Ar, Kr, Xe, and Hg ion bombardment) has a threshold of 25 to 30 ev (Stuart and Wehner, 1962). The target consists of a quartz dish 17 mm in diameter and 5 mm high. Supporting the dish is a metal disc to which the rf is applied. The dish is filled with the powder to be studied (Figure 1). Sputtering from the glass-covered lead to the metal disc cannot deposit much material on the sample because the target surface cannot see the lead and sputtered atoms stick to the tube wall. Very few of them would be deviated from straight-line flight to the wall by gas-scattering.

The plasma is excited and maintained by several hundred watts of rf power at 48 Mc/sec. Coupling to the plasma is achieved inductively by a loop around the glass sputtering chamber as shown in Figure 1. There must be a small amount of sputtering from the glass wall due to electric fields from the exciting loop. Such sputtered atoms could reach the sample. Control experiments with the plasma excited but no 2.5 Mc/sec ion bombardment indicated negligible deposition during our exposure times.

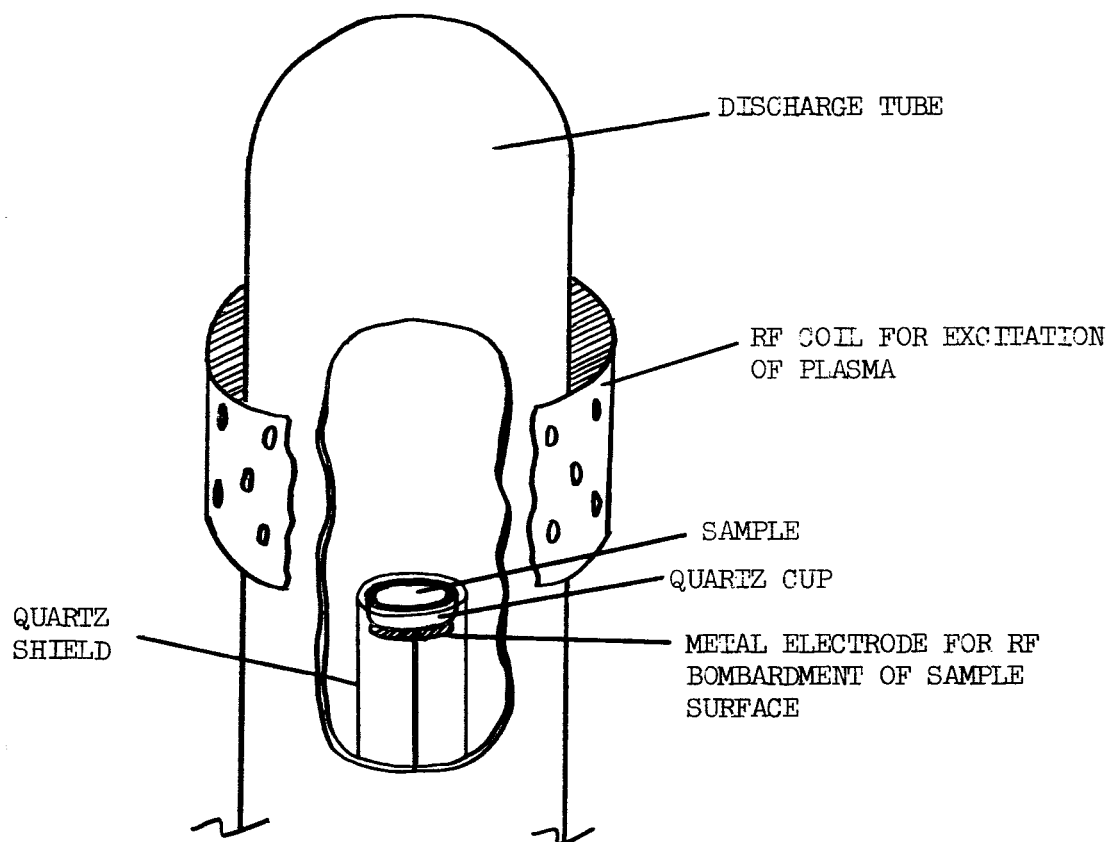


Fig. 1. Schematic of plasma bombardment system.

The relation of laboratory sputtering in our apparatus to actual solar-wind sputtering is as follows. We take a solar-wind flux of  $2 \times 10^8 \text{ H}^+ \text{ cm}^{-2} \text{ sec}^{-1}$  at 450 km/sec (1 kev) and  $3 \times 10^7 \text{ He}^{++} \text{ cm}^{-2} \text{ sec}^{-1}$  at the same speed (4 kev) as being representative of the current solar wind. Ancient fluxes may have been higher (Wilson, 1966). Our speeding up the bombardment rate by nearly eight orders of magnitude should be allowable as far as sputtering or darkening effects are considered because the lattice relaxation times are short ( $10^{-13} \text{ sec}$ ) relative to the periods between disturbances of surface atoms ( $10^{-1} \text{ sec}$ ). It is not possible to achieve simultaneous 1 kev  $\text{H}^+$  and 4 kev  $\text{He}^{++}$  bombardment in our plasma. In fact, the extracted ions are not mass-analyzed so in mixed hydrogen-helium discharges the ratio of the ions cannot be controlled. But in this energy range we have previously obtained data (Wehner et al., 1963a; KenKnight and Wehner, 1964, to be published) indicating useful approximations in comparing hydrogen and helium sputtering: He ions sputter four times as rapidly as protons at a given energy because of their greater mass; both hydrogen (up to 2 kev) and helium (up to 5 kev) sputtering increases nearly linearly with ion energy. Therefore we can express the sputtering contribution of solar-wind  $\text{He}^{++}$  in terms of  $\text{H}^+$ . The increase due to  $\text{He}^{++}$  is  $0.15 \times 4 \times 4 = 2.4$ . If the assumed solar-wind abundance of  $\text{He}^{++}/\text{H}^+ = 0.15$  is correct, then a flux of  $6.8 \times 10^8 \text{ H}^+ \text{ cm}^{-2} \text{ sec}^{-1}$  at 1 kev should give the same erosion rate as the actual solar wind. In averaging over the moon and various lunations, this flux should be further multiplied by factors:  $\frac{1}{2}$  for lunar night,  $\sec \theta$  for increased yields at oblique incidence,  $\cos \theta$  for reduced current density at oblique incidence. The average flux of an equivalent solar wind is then

$3.4 \times 10^8 \text{ H}^+ \text{ cm}^{-2} \text{ sec}^{-1}$  or  $1.7 \text{ C/cm}^2$  in  $10^3$  yr. Consideration of the partial deflection of the solar wind due to collective effects would be premature at our present level of knowledge of solar-wind dynamics. Magnetic deflection is improbable because the poles of a lunar dipole would be anomalously darkened and at least one pole would be visible from earth.

In our discharge the ions are mostly  $\text{H}_2^+$  (20 millitorr  $\text{H}_2$ ) plus some  $\text{H}^+$  and  $\text{H}_3^+$ . The ion energy varies during a cycle, the dc level of the voltage is 500 v. For hydrogen sputtering of a large number of metals by kiloelectron volt ions (KenKnight and Wehner, 1964, and to be published), we have found that molecular ions sputter just like independently incident atomic ions of the same speed. Thus the erosion due to  $1.7 \text{ C}$  of  $1 \text{ kev H}^+$  is equal to that of  $\frac{1}{2} \times 1.7 \text{ C}$  of  $2 \text{ kev H}_2^+$  ions. But our effective ion energy during the rf cycle is about 500 ev. Using the approximation of sputtering proportional to energy,  $10^3$  equivalent years require  $3.4 \text{ C/cm}^2$  of  $\text{H}_2^+$  ions at 500 ev. At  $1.7 \text{ ma/cm}^2$ , this dose is accumulated in 33 minutes in our apparatus. No correction for the admixture of  $\text{H}^+$  and  $\text{H}_3^+$  ions is necessary if it is accurate that molecular ions sputter like independent atomic ions and if sputtering is proportional to ion energy because, at a given applied voltage, each constituent of the ion  $\text{H}_n^+$  has energy  $E/n$ , but the whole ion contributes a share  $n \times E/n$  to the sputtering. Thus in this circumstance, a given number of hydrogen ions causes a fixed amount of sputtering, independent of the  $\text{H}^+:\text{H}_2^+:\text{H}_3^+$  ratios.

It is important to consider the surface temperature in view of possible thermal effects. At the stated current level and in the presence of the hot plasma, about  $0.9 \text{ w/cm}^2$  is dissipated in the sample surface. Several



independent methods have shown the maximum temperature attained at the insulator surface to be below 400°C. Conduction through the sample and radiation from the surface are estimated to be 0.3 and 0.1 w/cm<sup>2</sup>, respectively, while gas conduction (20 millitorr H<sub>2</sub>) could account for up to about 0.7 w/cm<sup>2</sup>. We observe weak bonding of the surface particles after bombardment for the equivalent of 10<sup>4</sup> yr or more. The temperature rise alone would not cause bonding; any cold welding must be due to sputtered material (Wehner et al., 1963b) or the sintering caused by crystal damage (Smoluchowski, 1966).

## 2. Reflectometer

The light reflection, polarization, brightness, and color characteristics of various sample surfaces were determined by the use of a specially designed reflectometer shown schematically in Figure 2. With this instrument a horizontal surface can be illuminated and viewed from angles of -90° to +90°. The surface is illuminated with a Bausch and Lomb microscope illuminator head using a General Electric No. 1630 spiral filament operated at reduced voltage. The incident light beam is formed by a two-lens system and reflected 90° by a front surface mirror onto the surface under study. This mirror arrangement allowed measurements to be made down to a mean phase angle of 2.5°. The spread in phase angles was 4.8°, mostly due to the size of the detector lens. The recent use of a narrower mirror and a slit in front of the detector lens permits measurements to phase angles less than 1° with a spread of 1.0°. The surface normal is chosen to be in the scattering plane so the phase angle

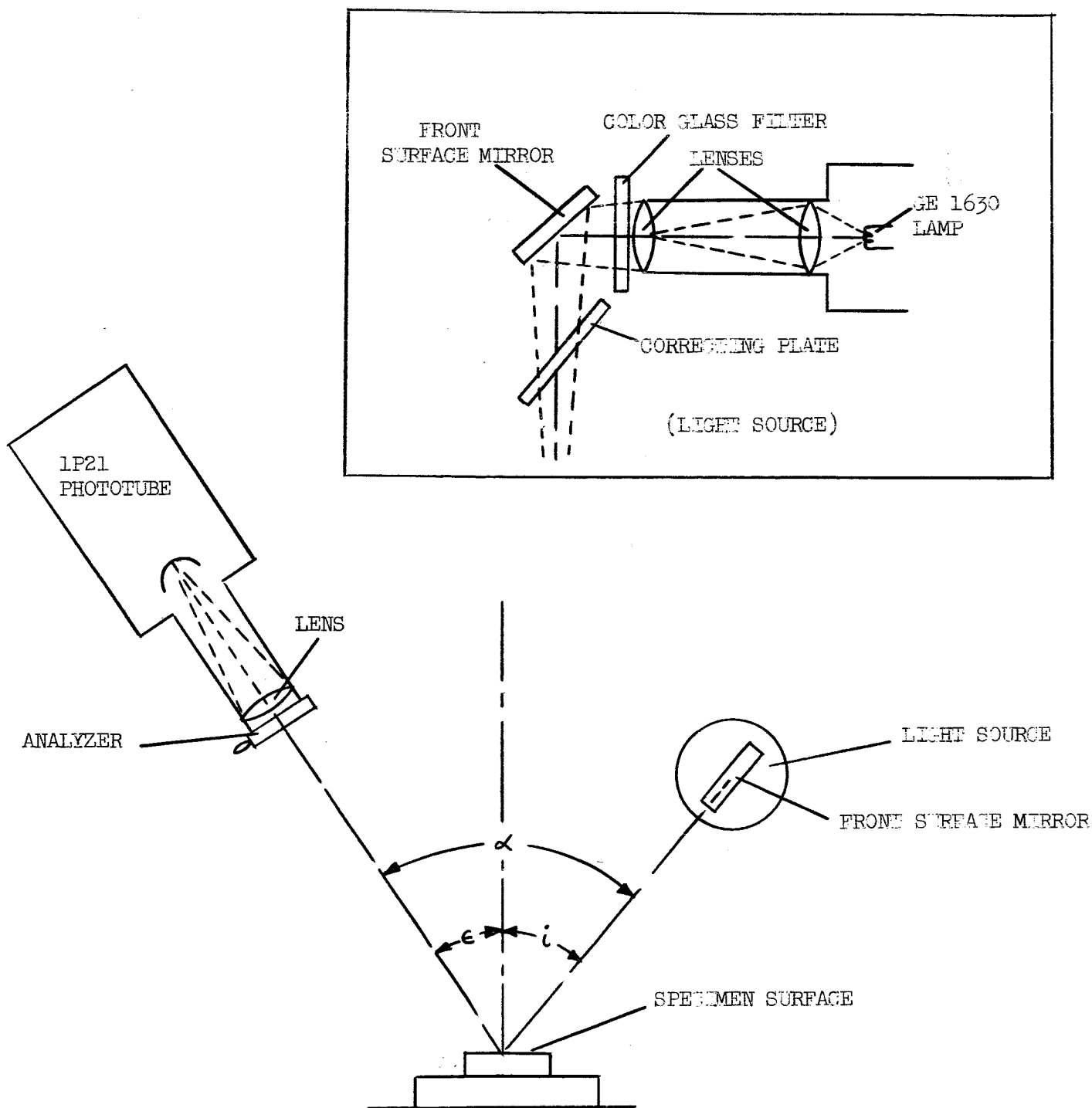


Fig. 2. Reflectometer used in photometric and polarimetric measurements.

is simply the sum of the angles of illumination,  $i$ , and of detection,  $e$ . The beam spot is 17 mm in diameter at the specimen stage. Provision is made for inserting Corning Color Glass Filters into the illuminating beam path between the last lens and the front surface mirror. The effective wavelengths of the filters are: ultraviolet 3700 Å, blue 4200 Å, green 5200 Å, red 6100 Å. The bandpass at half intensity for these approximately triangular peaks is about 350 Å in ultraviolet and 550 Å for the remainder.

The detector system employs a 1P21 phototube and one lens and sees a 3 mm diameter spot on the specimen surface when the detector is normal to the surface. Eastman Kodak Neutral Density Filters were used in the reflected light path just in front of the detector lens when measuring the lighter colored surfaces.

When the reflectometer is used for polarization measurements, an analyzer is attached to the end of the detector tube and an adjustable glass depolarizing plate is mounted in the path of the illuminating beam just below the front surface mirror. The depolarizing plate can be rotated azimuthally as seen along the light beam and tipped so as to remove the linear polarizations introduced by emission from the spiral filament and by reflection from the mirror. Adjustment is made with detector and light source facing each other on opposite sides of the reflectometer. The light passes straight through a neutral density filter which is placed perpendicular to the light beam at a position in the center of the reflectometer. The filter absorbs and scatters the incident light but should not change the polarization of the light transmitted in the forward direction.

Over the 3 mm circle of the filter viewed by the detector, the mean polarization in green light could be made less than 0.05%. In red or blue light the residual polarization was then found to be about 0.2% so that for measurements not demanding strictly unpolarized incident light (e.g., those near the phase angles of maximum polarization of the scattered light), comparisons at different wavelengths could be made without readjusting the tilting plate. In principle, one could adjust the tilting plate by measuring the reflection from a glass surface at the usual sample position and using the Fresnel formulas. But it was difficult to orient the surface normal to sufficient precision. The minimum phase angle for polarization measurements was about  $7^\circ$ . Later improvements have permitted measurements to  $4.5^\circ$ . The incident beam is depolarized for precision photometry to be reported below. The contributions to linear polarization of the incident beam nearly cancelled for most of the earlier photometry, and depolarization was omitted for convenience.

### 3. Criticisms of Equipment and Procedure

We freely admit the existence of limitations inherent in the data of this paper and group them here for the reader. Besides not simulating the effects of ballistic flights of sputtered atoms to great distances on the moon, there are effects peculiar to the reflectometer and to the method of sputtering.

The distance from sample to the detector lens or the light source mirror in the reflectometer is only 20 cm so the spot size viewed on the sample had to be small (3 mm). As a consequence, particles larger than 0.3 mm could not be studied without the effects of particle facets becoming

dominant. Even for particles smaller than 0.3 mm we believe we have detected effects due to facets in the form of small oscillations in the polarization curve as a function of phase angle  $\alpha$ . The oscillations occurred in the region of  $\alpha = 90^\circ$  to  $150^\circ$  where polarization of scattered light is largest. They were more marked if specular reflection from the mean surface was detectable. The oscillations became undetectable for the smallest particle sizes.

After showing that most of our sifted powder surfaces scatter light according to a modified Lommel-Seeliger law as given below, we were able to discover that a small amount of light was scattering into our detector from the quartz sample dish during the photometric measurements. This affected only the measurements we made for  $\epsilon = 30^\circ$  and  $60^\circ$  at large phase angles. The dish was shaded for polarimetry.

In polarization measurements, we detected an asymmetry in the reflectometer that was traced to gradients in the polarization of light emitted from the spiral filament and to misalignment of the filament. This alignment-gradient asymmetry has been greatly reduced in recent measurements by rotating the filament  $90^\circ$  about the light source axis. Like that from a hot cylinder of the spiral filament size, the emitted light is polarized toward the limb of the spiral with the electric vector parallel to the coil axis. The net polarization is 4.5% in green light. If the range in angles of incidence for the reflectometer were infinitesimal, the asymmetry would have been undetectable. For our finite  $\Delta i = 1.7^\circ$ , the asymmetry was important for angles of incidence within about  $20^\circ$  of glancing incidence. In particular, polarization measurements near  $\epsilon = 60^\circ$ ,  $\alpha = 120^\circ$ , which enter our analysis, were not affected because symmetry was observed in that vicinity.

In the presence of a hot hydrogen plasma there may be chemical and photochemical effects taking place in addition to specifically physical sputtering effects. While some control experiments were done in which no detectable darkening resulted from mere exposure to the plasma, such experiments cannot rule out chemical effects depending upon damaging, activating, or heating the sample surface in the presence of  $H_2$  gas. Further experiments with ion beams are needed to clarify this issue. But some experiments with helium ion bombardment resulted in darkening analogous to that caused by hydrogen ion bombardment. Therefore the main effects to be reported here must be due to physical sputtering.

The large ( $\sim 200$  v/mm) electric fields above our samples while drawing ions from the plasma seem to be capable of aligning surface particles. Wehner et al. (1963b) published photographs showing needles and other microscopic alignment features in a crust on  $Cu_2O$  that were aligned with the local surface electric field. These features were enriched in metal due to preferential loss of oxygen from the crust during Hg-ion bombardment. The brightness of this crust was markedly great when viewed at small phase angle but large angle of emergence, i.e., perpendicular to the metallic needles. This observation would correspond to limb brightening at full moon in the lunar case and be contrary to fact. The limb brightening was accompanied by a corresponding effect in polarization at the same angles: the electric vector of the emerging light was enhanced in the plane defined by the needles and the direction of emergence as though the needles were radiating like small dipoles. The actual polarizing mechanism involves

diffraction and can be inferred from the discussion of Hopfield (1966). This combination of limb-brightening and shift of the polarization at fixed, small phase angle as a function of angle of emergence is present, in strong correlation, to some degree for all our sputtered samples. It is especially marked for samples where there is an abundance of small particles available and for samples on which the particles become conducting. The importance of this alignment effect is that the polarization of the scattered light at large phase angles may have been affected by an unknown amount. Arguing against a major error is the fact that for sifted, unsputtered powders, the polarization curves as a function of phase angle for several angles of emergence closely coincide. After sputtering, the corresponding polarization curves differ at small phase angles but converge at larger phase angles ( $\alpha \approx 90^\circ$ ). Reliable results from our darkening experiments with an ion beam, where the surface electric field will be orders of magnitude smaller, are not yet available.

Large electric fields in the plasma sheath above our samples could conceivably affect our results in a second way if a sizable fraction of the sputtered atoms (or molecules, if any) were emitted as ions. Negative ions would be accelerated away through the plasma sheath, but positive ions would be returned to the sample surface. In other sputtering experiments with oxides in this laboratory, we have observed beams of energetic negative ions which we suppose are  $O^-$  ions. This phenomenon might be fairly general for insulators. The ionic component is very low for metals and semiconductors. The moon is commonly supposed to be charged positively to 10 v or more (e.g., Singer and Walker, 1962), due mostly to solar

ultraviolet light and the photoelectric effect. In that case, negative ions such as  $O^-$  would be retarded or returned to the lunar surface while positive ions would be accelerated outward to greater than the lunar escape velocity. Further experiments are needed on this point.

## C. RESULTS

### 1. Composition Dependence

Various igneous and metamorphic rocks, glasses, compounds, metals, a meteorite, and a tektite were subjected to simulated solar-wind bombardment. Not all of the materials studied are necessarily highly probable lunar surface materials. But among the rocks studied are six "standard samples of likely lunar rock types" proposed by J. Green (1965). This section is devoted to the consequences of varying sample composition while holding particle size and surface structure fixed. The size was generally less than  $44\ \mu$  and the surface was of low compaction. Only a few smooth, solid surfaces are markedly darkened by ion bombardment, e.g., solid  $BaTiO_3$ .

When oxides of Fe or Cu were bombarded by ions of either Hg or  $H_2$ , the presence of the free metal was demonstrated by powder diffraction analysis with x-rays. For these compounds, the oxide colors are quite different and color changes are very marked. For the (white) oxides of Al, Mg, and Ca, powder samples bombarded by hydrogen ions were negligibly to moderately darkened, the darkening increasing in the stated order. The metals could not be detected by x-ray analysis but such analysis is not very sensitive. Graphite powder is rapidly eroded by hydrogen-ion bombardment. About one carbon atom is removed per incident hydrogen ion in

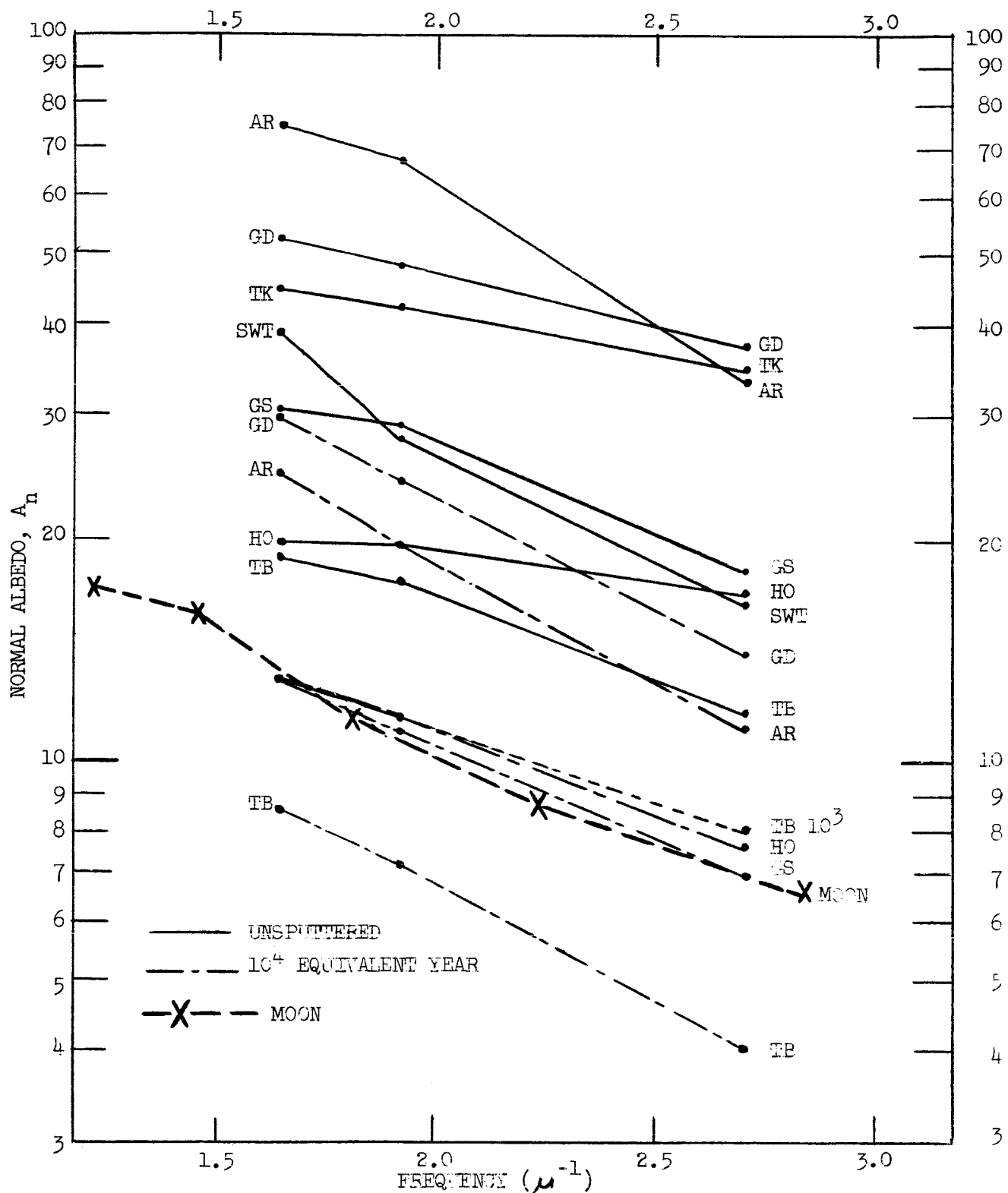


the plasma system. Aside from the ions (mostly  $H_2^+$ ),  $H_2$  gas is also available for reaction. At comparable energies, ions of He and Ar erode carbon at a rate slower by an order of magnitude and physical sputtering due to  $H_2^+$  should be even slower. Obviously reactive sputtering, with hydrocarbon formation, results from  $H_2^+$  bombardment. Probably for this same reason, SiC powder is rapidly transformed from a dark grey to a light tan shade.  $MgCO_3$  is not markedly affected by hydrogen-ion bombardment.

Let us here define "normal albedo" as the brightness of a sample measured at  $2.5^\circ$  nominal phase angle with a spread in phase angles from  $0^\circ$  to nearly  $5^\circ$ . The brightness is referred to a standard MgO surface, prepared in the usual way: collect an opaque ( $\sim 1$  mm thick) deposit of MgO smoke particles on a glass slide by burning clean Mg in air. In fact, the moon (Gehrels, et al., 1964; Van Diggelen, 1965), our powder samples, and even the MgO surface exhibit an abrupt increase in brightness at phase angles less than about  $3^\circ$ . The increase is due to the disappearance of shadows within the sample area at vanishing phase angle and detected photons enter and emerge from the scattering surface through the same opening. Beyond  $3^\circ$ , an important portion of the detected light enters and emerges through different openings. The "normal albedo", as defined, should correspond closely to lunar albedos that have been obtained by the old procedure of extrapolating to zero phase angle without taking into account the brightness increase below  $3^\circ$ .

The normal albedos  $A_n$  in red, green, and ultraviolet light for a number of bombarded and unbombarded rock powders are presented in Figure 3. On a plot of  $\log A_n$  vs frequency, the sample albedos decrease nearly linearly with frequency. This is particularly true after ion bombardment and is also true for the moon. Our photon frequencies do not coincide with those normally used for the moon but in a gross survey of color effects the slope of the  $\log A_n$  vs frequency curves may be used as a measure of color for any convenient frequency interval because of the linearity. In particular, the brightness of the mean moon decreases about 0.5 stellar magnitudes (X0.63) as the photon frequency is increased  $1\mu^{-1}$  (Harris, 1961) so that the color index for the moon is about  $0.5 \text{ mag}/\mu^{-1}$ , on the average. A color index based on just two frequencies is adequate to reveal when sample colors differ from lunar colors, but additional frequencies would have to be examined to establish when the colors were actually identical. For the present we only want to point out that most of our sample colors are quite different from the moon.

On the moon, individual features have albedos in green light that range from about 0.05 to 0.20, but the feature colors vary only from about 0.4 to  $0.6 \text{ mag}/\mu^{-1}$ . Our sample albedos before ion bombardment usually are in the range 0.2-0.8 for small particle sizes. Bombardment decreases the albedos into the lunar range by, or before, the equivalent of  $10^5$  yr. For larger particles of many rocks, the latter dose decreases the sample albedo below the lunar range.



AR ALTERED RHYOLITE      SWT SEMI-WELDED TUFF      HO HOLBROOK METEORITE  
 GD GRANODIORITE      GS GREENSTONE      TB THOLEIITIC BASALT  
 TK TEKITE

Fig. 3 Dependence of albedo upon photon frequency for rock powders and for the mean moon (Harris, 1961).

In contrast to the small range of lunar colors, our sample colors exhibit a wide range, both before and after bombardment. In Figure 4 we make an albedo-color diagram which shows the dispersion of lunar and sample colors. A similar diagram due to Sharonov is given by Fessenkov (1961). As a result of the albedo decreases and color changes due to ion bombardment, a given sample traces a "trajectory" in our diagram. Most of the samples become more reddish with bombardment, but exceptions are seen. There is no tendency for convergence of sample colors into a small range of colors, nor any tendency to adopt the lunar colors.

The albedos and colors of lunar features were obtained from the data of Gehrels et al. (1964). The albedos were obtained by fitting the phase function of Rougier (1933) for the whole moon to the photometric data of Gehrels et al. after removal of the Lommel-Seeliger dependence from the data of each (KenKnight, to be published). This procedure yields relative feature brightnesses of high accuracy since every photometric measurement enters with equal weight. Previous procedures weighted measurements at the smallest phase angles inordinately. The albedos are normalized to the albedo of the mean moon given by Harris (1961) by weighting the features according to the specifications of Gehrels et al. in order to compensate for a lack of bright features in their list. This normalization ignores the brightness increase at small phase angles as noted above so that sample and lunar albedos closely correspond. The color index was derived from UBV photometry for which the ultraviolet to green (U-V) frequency interval is  $1.01\mu^{-1}$ . On another instrument Gehrels et al. reported UGI photometry for which the U-G interval is  $0.91\mu^{-1}$ . The color

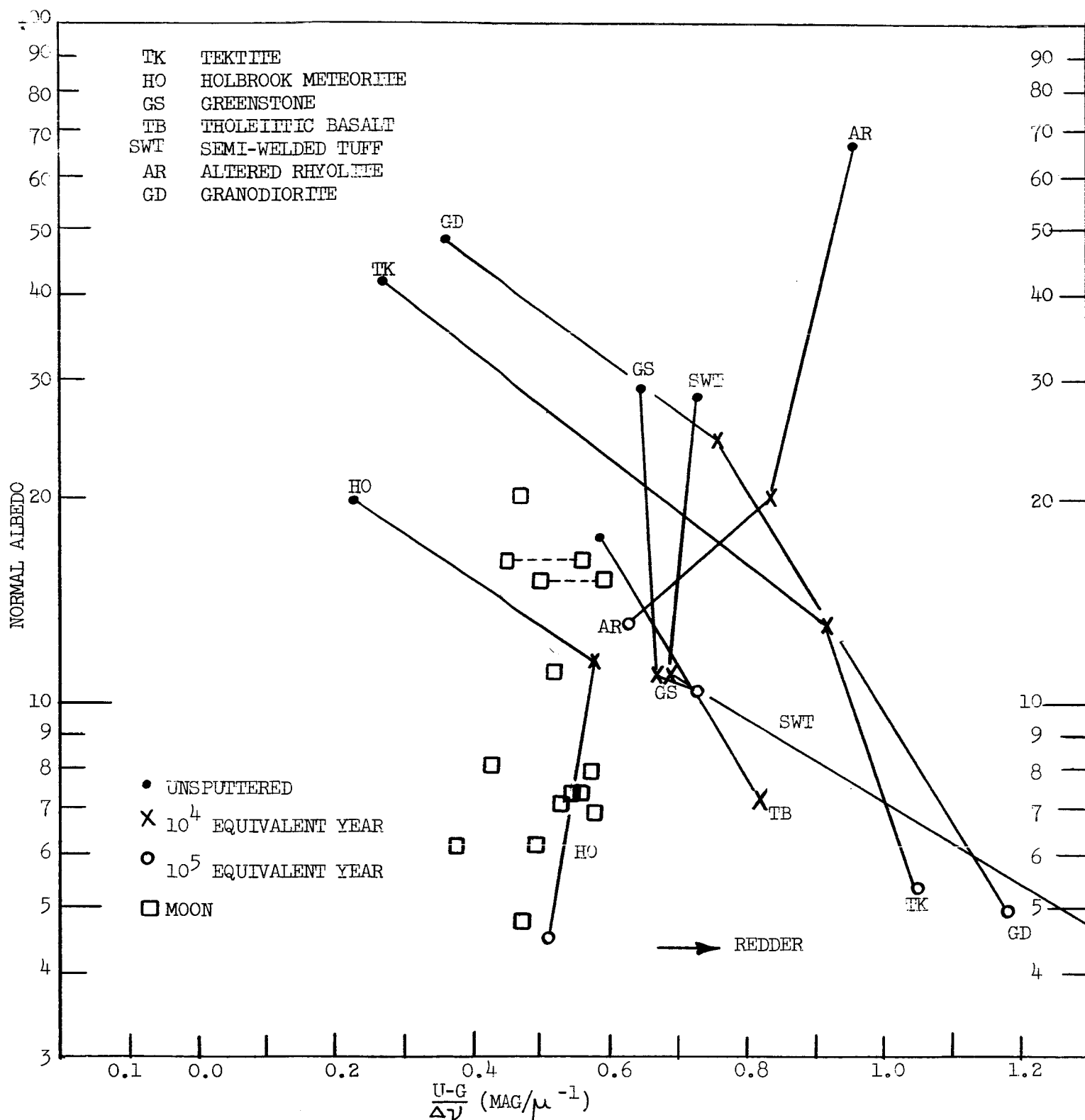


Fig. 4. Albedo-color diagram for samples of finely divided rock and for lunar features (Gehrels *et al.*, 1964). Line segments connect measurements on a single sample surface; changes are due to ion bombardment.

indices were in good agreement for the two systems for the darker features but were higher for the difficult bright features Copernicus and Clavius in the latter system. Both values are given in Table 2 and Figure 4. Agreement of published data on color of bright features is not good even for photoelectric determinations, as, for example, comparison of Kozlova and Glagolevskii (1958), van den Bergh (1962), and Gehrels et al. would show, but the small range of lunar colors centered on  $0.5 \text{ mag}/\mu^{-1}$  is certain (e.g., Fessenkov, 1961; Minnaert, 1961; Petrova, 1966).

The relatively good agreement (for this particular frequency interval) in Figure 4 between lunar colors and albedos and those of the bombarded powder of chondritic meteorite Holbrook is especially interesting because Holbrook powder is the least red sample in the group. The polarization of light scattered from it is also in good agreement with that observed from lunar features having the same albedo. A small admixture of meteorites is, of course, expected in the lunar surface. Perhaps an admixture of meteorites is influencing the lunar color so that it is less red than bombarded terrestrial rock powders.

If our color data are supported by further experiments and if lunar surface material is like terrestrial rocks, then a mixing process like the ballistic flight of sputtered atoms to great distances on the moon could be hypothesized to explain the very small dispersion in lunar colors. Yet despite gross global uniformity of color, there are sharp lines of color demarcation on the moon (e.g., Rackham, 1964). Color mixing at great distances could explain gross global uniformity co-existent with sharp lines of local color variations. Local sputtering between particles in a rough

TABLE 2. Albedos and Colors of Lunar Features as Derived From  
Gehrels et al. (1964) for Ultraviolet and Green Light

Region	Visual Albedo (%)	Color Index ( $\text{mag}/\mu^{-1}$ )
Mare Humorum	4.8	.475
Mare Tranquillitatis	6.2	.377
Mare Crisium	6.2	.494
Wood's Region	6.8	.579
Mare Serenitatis, East	7.1	.532
Mare Serenitatis	7.4	.548
Plato	7.4	.558
Palus Somni	7.6	---
Mare Imbrium	7.9	.571
Near Hrotensius	8.1	.429
Near Plato	11.2	.519
Copernicus	15.1	.50-.59
Nicolai	15.5	---
Clavius	16.3	.45-.56
Tycho	20.2	.473
Aristarchus	21.5	---

surface without a global mixing would, on the basis of our data, result in a great range of colors due to relatively minor regional composition changes.

The influence of composition upon the angular distribution of scattered light (the phase function) and upon the polarization of the scattered light is wholly characterized by particle albedos and by the opacity of particles of a given size. Reduced opacity results in some light being transmitted through the particles and a more diffuse scattering of light. Polarization is also decreased. These incidental influences of composition are treated below.

## 2. Influence of Surface Structure

We want to point out that the structure (the porosity) of a powder surface is important to its polarization properties but that there are no lunar optical data that permit us to decide confidently whether the surface is near maximum or minimum density. A large density is to be expected if the sequence of secondary impacts resulting from meteoritic impact culminates in a surface crushing action or if seismic disturbances cause the surface particles to settle. A low density might result if, for example, charging of micrometeoritic secondary particles causes deposition at low velocity. A mechanism resulting in cementation of the surface particles would then make a low surface density especially probable. Near a phase angle of  $90^\circ$ , the magnitude of the degree of polarization may increase more than 30% due to jarring a sifted powder sample so as to compact it. Moreover, in this circumstance the phase angle  $\alpha_+$  at which the maximum degree of polarization  $P_+$  occurs tends to shift to a larger value so that  $P_+$  may increase by 50% due



to compaction. We have observed  $\alpha_+$  as small as  $80^\circ$  on low-density surfaces and that it may increase to  $110^\circ$  upon compaction. The phase angle  $\alpha_+$  also increases as albedo decreases. Because of instrumental difficulties discussed earlier, we hesitate at this writing to discuss lunar surface compaction on the basis of the phase angle  $\alpha_+$ .

Above a certain particle size, the surface structure of a powder is not ambiguous. As pointed out by Hapke and Van Horn (1963), only sufficiently small particles can form a low-density structure while larger particles overcome interparticle forces and assume "gravel-pile packing". For most powders in (humid) air and subject to the force of earth's gravity, the critical particle size is 15 to  $20\mu$ . On the moon the critical particle size is not known because of the uncertain interparticle forces. But since the force necessary to support a particle of size  $D$  increases as  $D^3$ , allowance for a sixfold decrease in surface gravity and for a tenfold increase in interparticle forces allows only a fourfold increase in the critical particle size. Since Hapke and Van Horn believed that the photometry of the moon was not compatible with extensive "gravel-pile packing", they thus estimated that  $60\mu$  might be an upper limit to the particle size that is dominantly present in the lunar surface layer. We will now discuss all the remaining lunar optical properties that might permit some statement about surface compaction.

Hapke (1963) offered the suggestion that the brightness of individual lunar features is governed by a relation of the form

$$I(i, \epsilon, \alpha) = L(i, \epsilon) F(\alpha) \quad (1)$$

where the function  $L(i, \epsilon)$  is the Lommel-Seeliger function

$$\begin{aligned} L(i, \epsilon) &= (1 + \cos \epsilon \sec i)^{-1} \\ &= \cos i / (\cos i + \cos \epsilon) \end{aligned} \tag{2}$$

and where the second function  $F(\alpha)$  was separated into another product

$$F(\alpha) = S(\alpha) \times B(\alpha) \tag{3}$$

The function  $S(\alpha)$  describes how an average particle scatters light and  $B(\alpha)$  results from shadowing within a tenuous surface of small, opaque particles. Since Hapke gave explicit expressions for  $S(\alpha)$  and  $B(\alpha)$ , he compared the product function  $L(i, \epsilon)F(\alpha)$  to photometric data on lunar features but did not test the validity of his factorization explicitly. The recent photoelectric data of Gehrels, Coffeen, and Owings (1964, henceforth called GCO) have been re-analyzed (KenKnight, to be published) to test this factorization with the result that the factorization is, indeed, a valuable approximation for lunar features. Briefly,  $F(\alpha)$  should be symmetric about  $\alpha = 0$  so multiplying the intensity data by  $L^{-1}(i, \epsilon)$  should result in identical curves for positive and negative phases. A representative result is given in Figure 5. It may be seen that after multiplication by  $L^{-1}(i, \epsilon)$ , the data points on the brightness of a small region in Mare Transquillitatis for positive and negative phases lie on one curve to the 5% precision inherent in the data. In what follows we will argue that the moon is a good Lommel-Seeliger scatterer but that this does not specify the surface compaction.

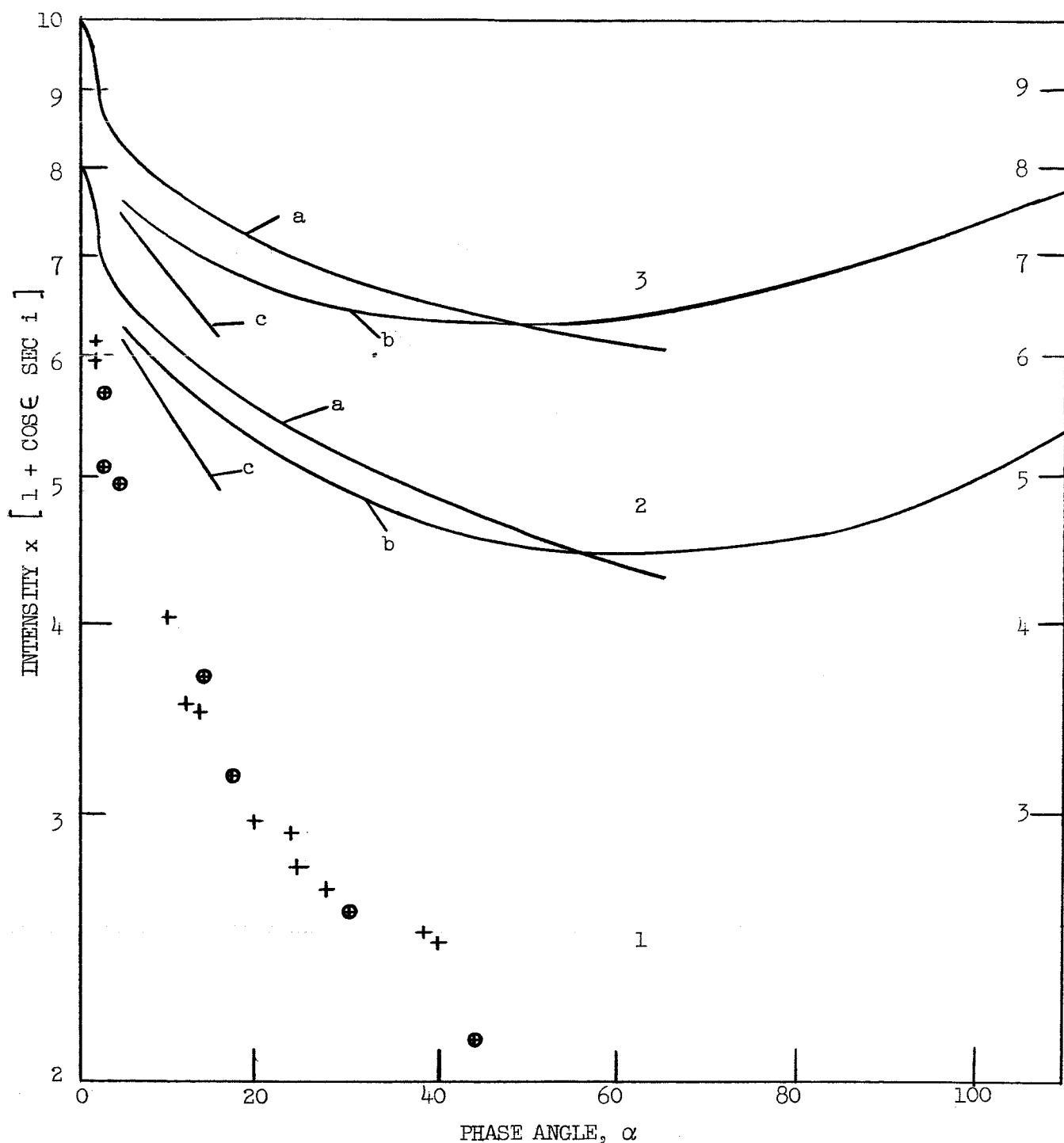


Fig. 5 Photometric functions  $F(\alpha)$  in green light of: 1) Mare Tranquillitatis, latitude  $39^{\circ}3'$ , according to Gehrels, *et al.* (1964), 2) Sifted  $10\text{-}20\mu$  tholeiitic basalt powder,  $A_n = 0.107$ , 3) Same powder compacted by shaking,  $A_n = 0.110$ . Curves (a) are for  $\epsilon = 0^{\circ}$ , (b) for  $\epsilon = 50^{\circ}$ , (c) for  $\epsilon = 50^{\circ}$  with light source between detector and the surface tangent plane. Curves (a), (b), and (c) are not arbitrarily placed but are related by limb-darkening effects. The circled points in (1) correspond to curves (b); the others correspond to curves (c).

If a powder surface is a Lommel-Seeliger scatterer in the sense of (1), then viewing the sample normal to its surface or from an oblique angle with  $\alpha = 0$  should reveal an identically bright sample because  $L(i = \epsilon) =$  constant. In Figure 5 a sample of basalt powder is shown to be slightly darker when viewed obliquely. The sample that was sifted for minimal compaction was 5% darker at  $\epsilon = 50^\circ$  than at  $\epsilon = 0^\circ$  whereas the sample that was purposely jarred for compaction was 10% darker at  $\epsilon = 50^\circ$  than at  $\epsilon = 0^\circ$ . Secondly, if these surfaces were Lommel-Seeliger scatterers, then the curves in Figure 5 for  $\epsilon = 0^\circ$  and  $50^\circ$  should have the same shape and the shape should be independent of the sign of the phase angle. In this test the sifted surface is again superior to the compacted one as a Lommel-Seeliger scatterer, but the function  $I \times L^{-1}$  for  $\epsilon = 50^\circ$  becomes progressively greater than that for  $\epsilon = 0^\circ$  at large phase angles. Unlike the Mare Tranquillitatis region, which is also viewed obliquely, a reversal of the sign of the phase angle at  $\epsilon = 50^\circ$  does not give identical curves for the basalt sample after multiplication by  $L^{-1}$ . Therefore the dependence of the brightness of the basalt powder sample in Figure 5 upon the angles of incidence and emergence is imperfectly described by  $L(i, \epsilon)$ , though the discrepancies are less than 10%. Darkening of such samples by sputtering invariably improves the agreement between the  $\epsilon = 0^\circ$  and  $\epsilon = 50^\circ$  curves. The laboratory data of Figure 5 were measured to 0.1% precision and are free from the error of light scattered from the sample container mentioned in an earlier section.

The darkening of the powder sample at oblique emergence angle for a given small phase angle would correspond in the lunar case to a slight limb-darkening at full moon. While the lunar limb-darkening is small, the brightness of a given feature at full moon cannot be used to decide whether the feature is a Lommel-Seeliger scatterer. Only a comparison of different features can be made; any statement about limb-darkening makes some assumption about equality of albedos for similar features.

Similarly, because of the very small range in  $\epsilon$  for a given lunar feature during the year (libration), it is not feasible to decide whether a given feature is a Lommel-Seeliger scatterer on the basis of comparing photometric curves for differing  $\epsilon$  on the given feature. Again, comparison might be sought for similar features. The data of GCO reveal that for 13 lunar features of various types, the variation in the shapes of  $F(\alpha) = I \times L^{-1}$  are so small as to be scarcely distinguishable in the interval  $5^\circ < |\alpha| < 50^\circ$ . Furthermore, if one assumes (1) holds for every lunar area, then the brightness of the whole moon is given by

$$T(\alpha) = \left[ 1 - \sin \frac{\alpha}{2} \tan \frac{\alpha}{2} \log \cot \frac{|\alpha|}{4} \right] \times \bar{F}(\alpha) . \quad (4)$$

When the Lommel-Seeliger dependence of (4) is removed from the data of Rougier (1933), the mean phase angle function  $\bar{F}(\alpha)$  is in very good agreement with all the lunar features of GCO with the possible exception of the bright ray crater Tycho. For Tycho the function  $F(\alpha)$  seems to decrease less rapidly with increasing  $|\alpha|$ . This comparison of photometric curves for

differing  $\epsilon$  (on different features) would suggest that all the features are good Lommel-Seeliger scatterers. Indeed, all the features pass the phase-angle symmetry test of Figure 5 equally well.

We now emphasize that the two sample surfaces of Figure 5 were of quite different compaction but that a low compaction did not grossly improve the sample behavior as a Lommel-Seeliger scatterer. It seems more probable that the remarkable symmetry of the lunar data in Figure 5 is related to that surface structure that governs the shape of  $F(\alpha)$ .

Very few of the data of GCO extend beyond  $|\alpha| = 50^\circ$  but the data of Rougier extend from  $\alpha = -130^\circ$  to  $\alpha = +150^\circ$ . The function  $\bar{F}(\alpha)$  continues the nearly exponential decrease of Figure 5 so that, for example,  $\bar{F}(120^\circ)/\bar{F}(5^\circ) = 0.155$ . In contrast to such a great decrease of  $\bar{F}(\alpha)$ , the comparable ratio for the basalt powder sample is approximately unity. The powder sample is already of sufficiently low albedo to agree with an average lunar region. Darkening of the sample by sputtering tends to reduce the brightness at large phase angles relative to small phase angles (stronger backscatter) but in no case have we observed a ratio  $F(120^\circ)/F(5^\circ)$  smaller than 0.5. We conclude that the exponential decrease in the lunar  $F(\alpha)$  at large phase angles requires a rough macrostructure which shadows a large fraction of the (powder) surface. It seems reasonable to suggest that a rough, shadowed structure on a centimeter to decimeter scale, such as was revealed in the Luna 9 photographs, can satisfy this demand. Our sample surfaces were essentially smooth within the viewed area, but a rough macrostructure would constitute a distribution of surface orientations. Some of the surface elements make no contribution at large phase angles. Therefore

the lunar  $F(\alpha)$  falls far below that measured for smooth powder samples. Clearly, then, no evidence on whether the microstructure is that of a compacted powder or not is forthcoming from photometric data at large phase angles because the macrostructure is not intimately known. On the other hand, the uniformity in the function  $F(\alpha)$  for many features suggests that the macrostructure hardly varies from one feature to another.

At small phase angles, the effects of shadows in a macrostructure should become negligible in comparison to the shadows in a microstructure. The theory of Hapke (1963) was intended to treat this case of small phase angles. Unfortunately, various mistakes in conception and calculation were made: entrance and emergence of the photon is treated asymmetrically; his function  $B(\alpha)$  does not follow from the indicated integrations; entrance and emergence of the photon through the same surface opening or adjacent ones is treated inadequately.

In any case, the theory of Hapke ignores multiple scattering and diffraction so that the shape of the photometric function does not depend explicitly on photon wavelength, contrary to the observation of GCO that the lunar backscatter peak is stronger at shorter wavelengths (lower particle albedos). What they noted was that the moon becomes more red with phase according to the relation (corrected for the color of sunlight):

$$(U-G) = +0.496^m + 0.0036 |\alpha| .$$

This says that the moon is brighter in green light than in ultraviolet light by about 0.5 stellar magnitudes (by 1.62) at full moon and that the ratio is

increased by another 14% at  $|\alpha| = 40^\circ$ . In Figure 6 we show that an effect of this magnitude and sign is present in scattering from a powder, in this case from a metamorphic rock commonly called greenstone. It is an example of a powder having relatively opaque particles with rough facets, but is otherwise undistinguished. The steeper descent of  $F(\alpha)$  for the unsputtered or sputtered samples when measured in ultraviolet light instead of green light amounts to an increase in the ratio of brightnesses of roughly 14% at  $|\alpha| = 40^\circ$ . The fact that the symmetry of the curves in Figure 6 is not identical in the different colors on the same surface resulted from moving the sample between changing filters in order to make the albedo determinations. Therefore slightly different sample areas were viewed.

The way to show that this dependence of the photometric function upon color is due to multiple scattering and negligibly due to diffraction is to notice that the extent of multiple scattering depends upon albedo but not upon photon wavelength. Therefore at different wavelengths for which the albedo is the same, the measured photometric function shapes should be the same if multiple scattering is the cause of this color-phase effect. In Figure 6, the unsputtered sample has an albedo of 0.18 in ultraviolet light (curve 1c); after sputtering for the equivalent of  $10^4$  yr, the sample has an albedo of 0.13 in red light (curve 2a); the function shapes are closely similar. The analogous curves 2c and 3a in Figure 6 are also closely similar to each other; the respective albedos are 0.068 and 0.062.



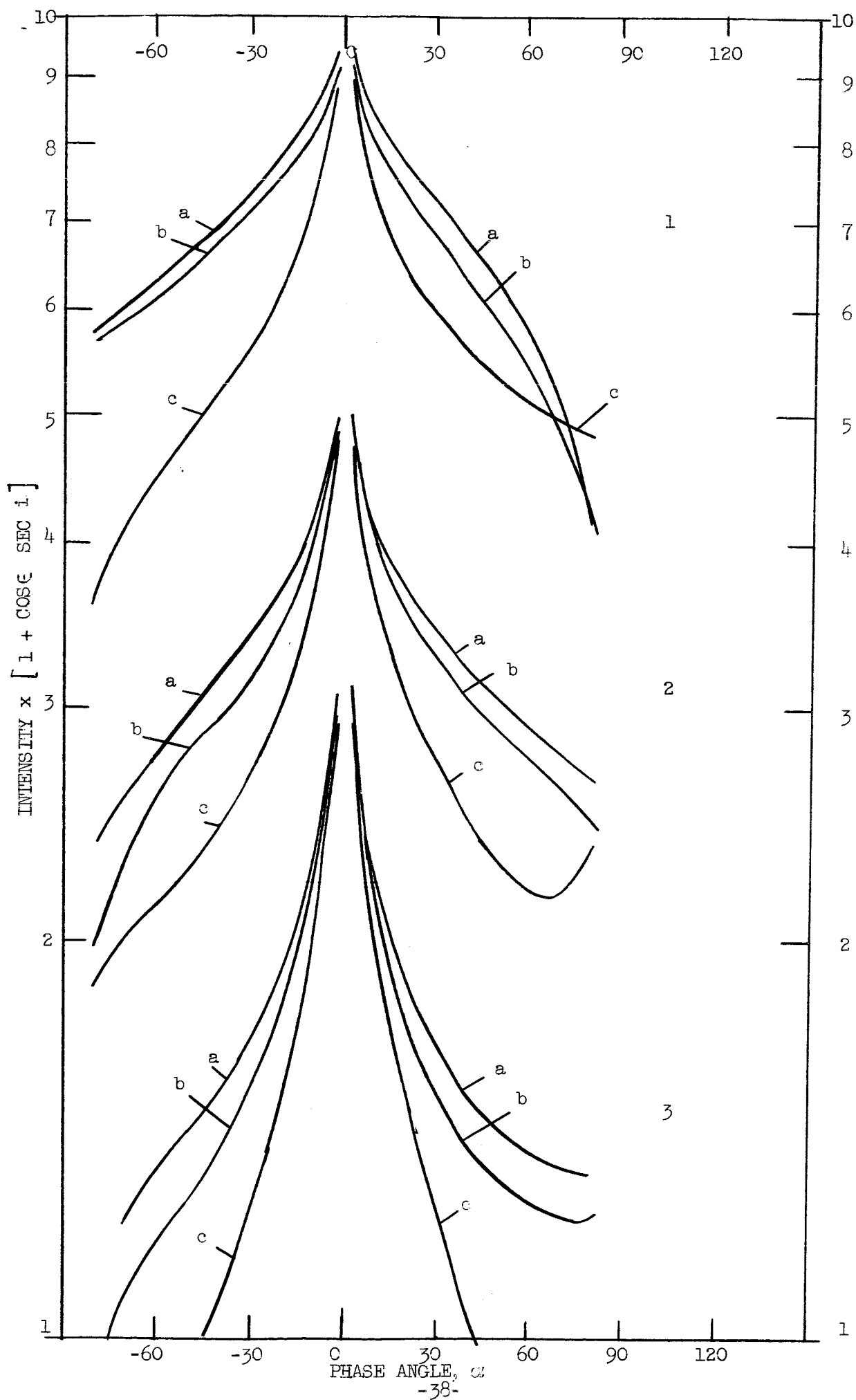


Fig. 6. Photometric function  $F(c)$  at  $c = 0^\circ$  for sifted  $0-20 \mu$  greenstone powder. The function depends markedly on the wavelength of the scattered light. (a) Red light, (b) Green light, (c) Ultraviolet light. 1) Unspattered, 2)  $10^4$  equivalent year, 3)  $10^5$  equivalent year.

We have found a similar result for larger particle sizes. Since the surfaces are compacted for the larger particle sizes, this effect therefore does not require an underdense surface structure. In particular, the dependence of lunar color upon phase does not imply anything about the lunar surface compaction.

One of the attractive features of the theory of Hapke was the idea that the steepness of the descent of the photometric function  $F(\alpha)$  near  $\alpha = 0$  should be related to the compaction of the scattering surface. In Figure 5, the photometric function for the basalt powder sample is seen to have two fairly distinct regions: an abrupt drop in brightness to  $|\alpha| \cong 3^\circ$  followed by a more gentle decline at larger phase angles. Most of the breadth of the peak at small phase angle is due to the angular resolution of the reflectometer:  $\Delta\alpha = 1.0^\circ$ , divided into  $\Delta\epsilon = 0.3^\circ$  and  $\Delta i = 0.7^\circ$  in approximately rectangular responses. The laboratory data in Figure 5 for  $|\alpha| \geq 1^\circ$  were measured in the usual way with the reflectometer. The data for  $|\alpha| \leq 5^\circ$  were checked with a beam-splitting arrangement and the point for  $\alpha = 0$  was thus added.

The steep decrease of the lunar  $F(\alpha)$  for  $0 < |\alpha| < 5^\circ$  was first established in GCO, then extended to additional features by van Diggelen (1965), who also reviewed the earlier data in which this opposition effect was suggestive. The calibration of van Diggelen depended upon GCO, but in re-analyzing the data of GCO we found such a large scatter in their data for  $|\alpha| < 3^\circ$  that we can only estimate  $1.25 < F(0^\circ)/F(5^\circ) < 1.5$ . Variations in the opposition effect with type of lunar feature cannot be confidently established from these data. By comparison, the ratio  $F(0^\circ)/F(5^\circ)$  was

estimated to be in the range 1.6 to 2.2 by GCO and van Diggelen, which seems to be an overestimate. The ratio is 1.23 for the sifted powder of Figure 5 and only 1% less for the compacted sample. Both of these ratios are apt to be underestimated due to the fact that our angular resolution  $\Delta\alpha = 1.0^\circ$  is about three times larger than that of the sun-moon-observer system. Further experiments with narrower angular resolution and further lunar observations are needed before any decision can be made on whether the opposition effect is modified by surface structure.

At phase angles much larger than  $5^\circ$ , surface shadows affect the brightness of the moon. But one might suppose that there exists a small angular region having  $|\alpha| > 5^\circ$  for which the effect of shadows in the macrostructure of the lunar surface is small in comparison to the effect of shadows in a microstructure. No unique angular region is obvious from the lunar data. Then one should choose an interval as small as is consistent with an experimentally significant change in brightness. Let us consider the decrease in brightness from  $|\alpha| = 5^\circ$  to  $20^\circ$ . In this angular range our use of an angular resolution of  $\alpha = 4.8^\circ$  should not have significantly affected the ratio  $F(20^\circ)/F(5^\circ)$ .

In Figure 7 are given the results of our measurement of  $F(20^\circ)/F(5^\circ)$  for the MgO reference surface (a nearly diffuse scatterer), for greenstone powder (an example of strong backscatter), for tektite powder (an example of a powder whose particles are fairly translucent), and for basalt powder (opaque powder particles with shiny facets). Darkening of these powders generally decreases  $F(20^\circ)/F(5^\circ)$ , i.e., backscatter is stronger.

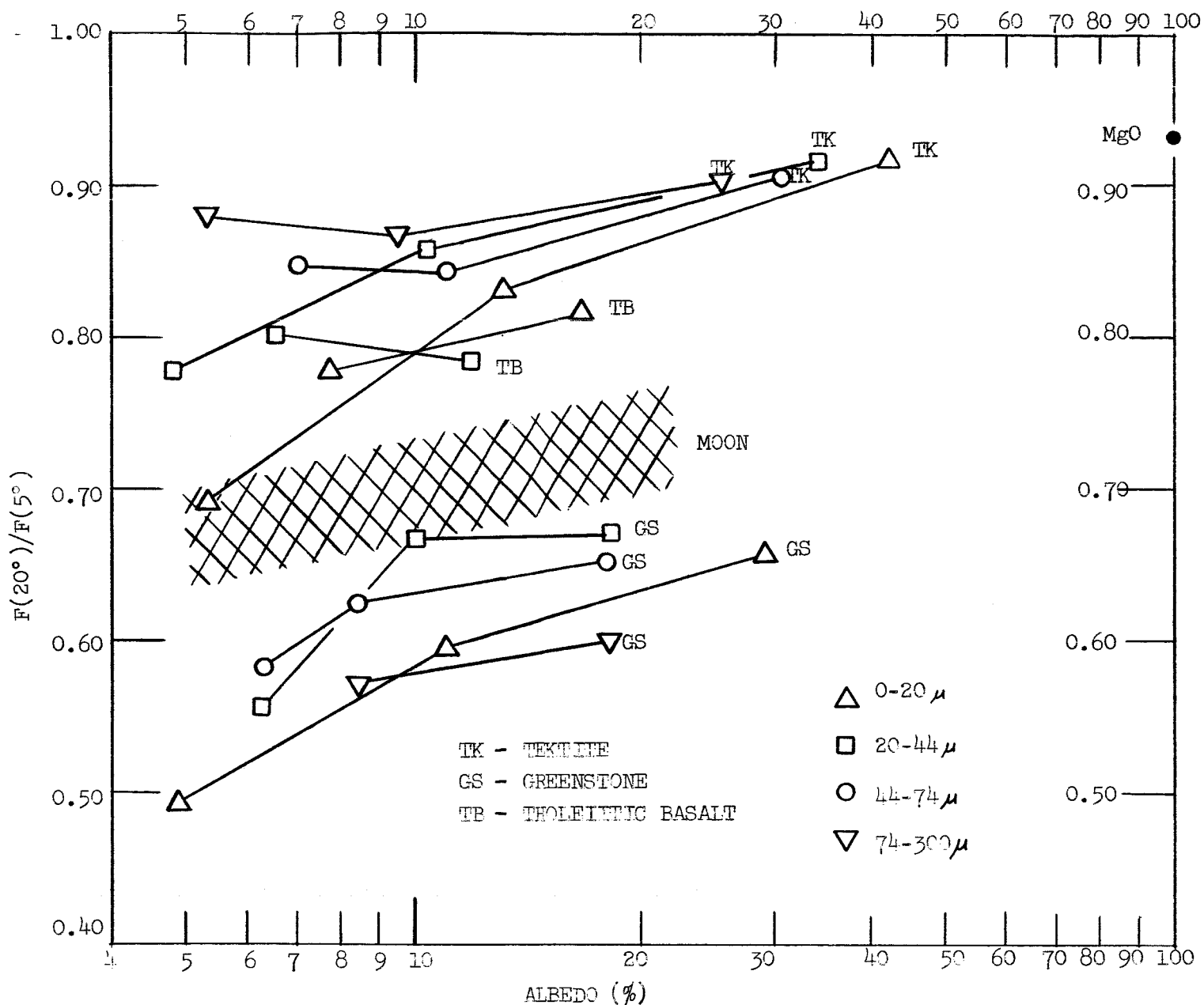


Fig. 7 Decrease in the photometric function  $F(\alpha)$  from  $|\alpha| = 5^\circ$  to  $20^\circ$  for green light for powder samples of various particle sizes and composition, and for the moon. Measurements on a surface whose albedo was decreased by sputtering are connected by line segments.

Some exceptions are seen for the larger size ranges of tektite powder. These samples tend to develop glazed, strongly reflecting facets. The same shiny facets are observed in all size ranges for tholeiitic basalt. Apparently for that reason, the values for basalt lie slightly above the range of values indicated for the moon in Figure 7. For the moon, the decrease in  $F(\alpha)$  is 0.70 in this angular range according to the data of Rougier. The possible variations in this ratio were considered on the basis of the re-analyzed data of GCO. Tycho,  $A_n = 20.2$  from Table 2, exhibits a decrease of about 0.77. The darkest lunar features may have a slightly stronger decrease than 0.70.

From Figure 7 we see that the steepness of the brightness decrease from  $|\alpha| = 5^\circ$  to  $20^\circ$  cannot be used to infer whether the lunar dust is compacted or not because compacted surfaces can be stronger backscatterers than the moon and low-density surfaces, even of opaque particles, need not be strong backscatters. In view of the indication that the presence of strongly reflecting facets leads to the weaker decrease in  $F(\alpha)$ , in the case of basalt, it seems probable that multiple scattering crucially affects the steepness of the brightness decrease in this range of phase angles. Multiple scattering is, of course, the basic reason for the diffuse scattering characteristic of MgO.

Finally we turn to a polarization phenomenon which also cannot be used to infer the composition or compaction of the lunar surface. It does, however, rule out a strongly metallized surface and does imply a powdery lunar surface. Sunlight scattered from the earth and its atmosphere is polarized. When this "earthshine" is observed on the dark

hemisphere of the moon from the earth ( $\alpha \approx 0$ ), a small polarization remains. Let us define R as the ratio of outgoing to ingoing degree of polarization and refer to it as the depolarizing ratio. While R is the directly measurable polarization parameter, we found for a large number of powders that  $R = KA^{-0.6}$ , where A is the sample albedo and K is a coefficient that hardly varies with sample composition, particle size, or compaction. In order to better display the small differences in K that do arise, we shall study the variable  $RA^{0.6}$ . The results from measurements of the depolarizing ratio in green light at  $\alpha = 5^\circ$  and of the sample brightness at the same angle relative to the MgO standard are presented in Figure 8. For these measurements at  $\alpha = 5^\circ$ , the variable  $RA^{0.6}$  hardly ranges below 0.06 or above 0.09 for a group of powders that includes underdense and compacted surfaces, opaque and transparent particles, small and large particles, sputtered and unsputtered surfaces. A notable exception is a pair of measurements on 20-44 $\mu$  Fe powder for which  $RA^{0.6}$  is about four times larger and therefore not shown in Figure 8. For sifted Fe powder, A was 0.153 and  $RA^{0.6}$  was 0.271, while for compacted Fe powder they were 0.183 and 0.310, respectively, at  $\alpha = 5^\circ$ . The sputtered powder samples had been exposed to the atmosphere for several months when this series of measurements was made so that if these samples were once enriched in metal, they presumably were oxidized by the time of measurement. The unsputtered powder samples were prepared according to the procedure of the subsequently sputtered samples and should correspond to "original samples".

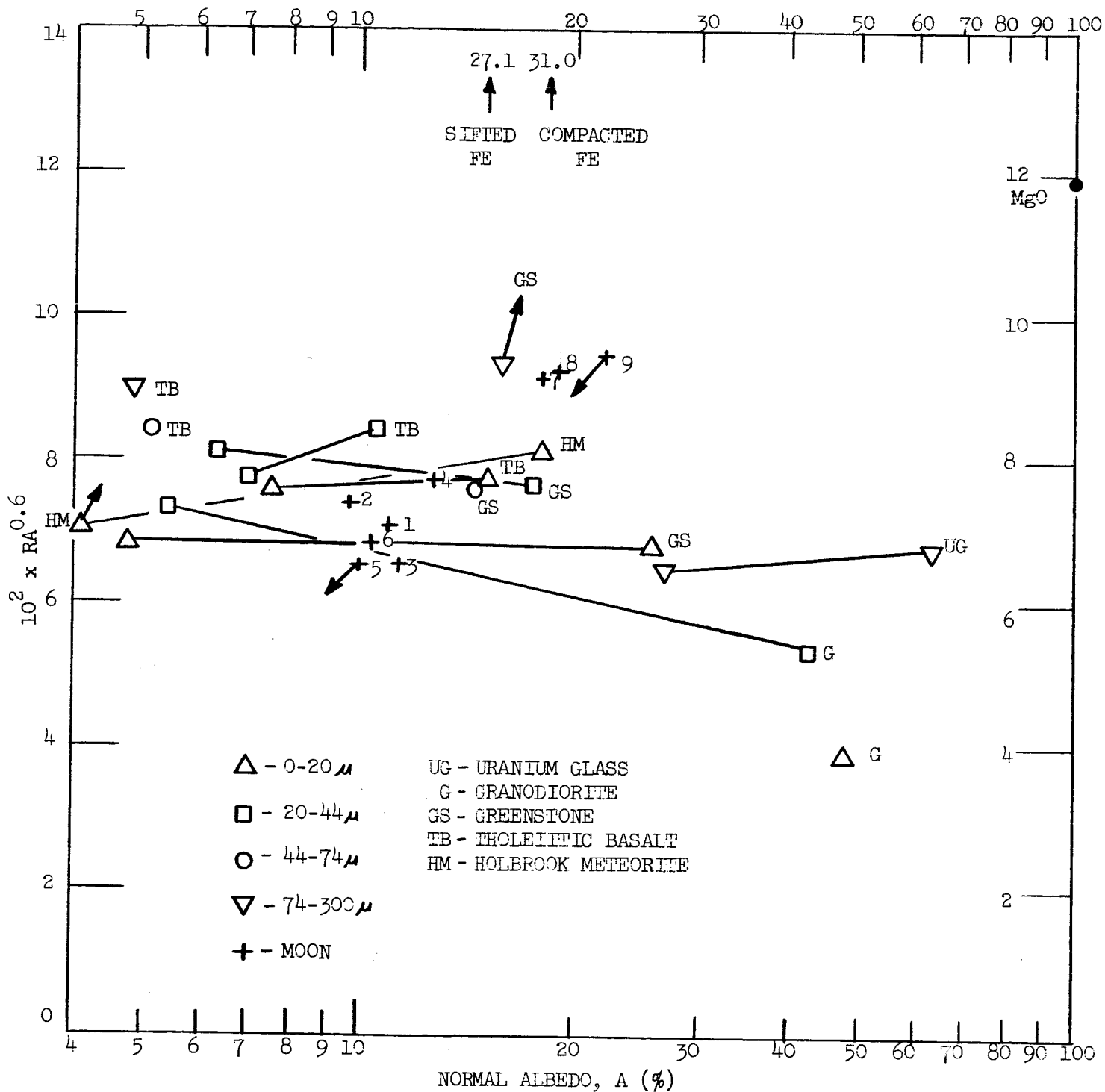


Fig. 8 Measurements of the depolarizing ratio  $R$  for various powder surfaces for which the albedo in green light is also known. Lunar values are due to Dollfus (1955). Line segments indicate surfaces darkened by sputtering. Vectors indicate the corrections discussed in the text that are necessary to put the laboratory and lunar measurements on the same basis.

The polarization of the earthshine was measured by Dollfus (1955, 1961) for 9 regions of the moon for which he also determined the albedo. From an estimate for the polarization of the earth's scattered light, he derived values for R which indicated a roughly inverse dependence of R upon A. He compared these R and A values to those of various substances and concluded that only powdery, opaque substances (especially volcanic ashes) gave satisfactory agreement. His tabulated lunar values are shown in Figure 8.

Before drawing final conclusions from comparison of our measurements to those of Dollfus we must consider the effects that result from our measurements being at  $\alpha = 5^\circ$  as compared to Dollfus'  $\alpha \approx 0^\circ$  and whether the albedos of Dollfus are accurate. We decline to discuss the estimate of the polarization of the earth's light made by Dollfus (0.33 at quadrature). Since the brightness of both the powder surfaces and that of the MgO reference surface both increase abruptly upon approaching  $\alpha = 0^\circ$ , we estimate that the value for A should be increased by 7% for the dark powder samples and be changed negligibly for the brighter samples. The value for R was also measured at  $\alpha = 10^\circ$  for many samples and at larger phase angles for certain samples. For other than the sample of Fe powder, R increases slowly toward  $\alpha = 5^\circ$  so that increases in R from 2% (for dark samples) to 10% (for lighter ones) are suggested by extrapolation. The small changes in the location of two points are shown by vectors in Figure 8. There are three regions studied by Dollfus that overlap areas studied by GCO from which the albedos of Table 2 are derived. Those three albedos of Dollfus are larger by a factor 1.6 with only 5% scatter. But if the



albedos of Table 2 are to be revised upward by a factor of, say, 1.4 when account is taken of the opposition effect, then the albedos of Dollfus would have to be decreased only by a factor 0.88 to bring them into correspondence to our sample albedos at  $\alpha = 0^\circ$  as corrected above. The change in the position of the lunar points in Figure 8 was calculated for an albedo decrease of 0.9 and the shifts are indicated by vectors. Albedo decreases larger than 0.9 would give proportionately larger shifts in the lunar points of Figure 8. We may conclude from Figure 8 that the lunar depolarizing ratio is in good agreement with a great range of terrestrial powder samples and affords little or no information about lunar composition and surface compaction. The possibility still exists that measurements of the depolarizing ratio made on sputtered samples not exposed to air might show that sputtering tends to enhance metal in the sample surface (increase  $RA^{0.6}$  markedly). In that case it might become necessary to consider why the lunar data agree with (oxidized) terrestrial rock powders.

### 3. Influence of Particle Size

Aside from the particle size effects which are mentioned in the above sections and which give no possibility of deciding what particle sizes are scattering light at the lunar surface, the effect of particle size upon polarization of the scattered light needs to be discussed. However, the conclusions expressed in our Eighth Quarterly Report have not been modified and the whole discussion need not be repeated here.

Briefly, we found that two parameters of the polarization near phase angle  $\alpha = 90^\circ$  equivalently imply scattering from a lunar powder containing particles mostly less than 0.1 mm in size. The large particles dominate the contribution to the polarization. Measurements on samples containing a quantity of small particles sufficient to significantly change the sample albedo showed that the polarization was equivalent to that from a sample of large particles only. The polarization index P depends upon sample albedo A according to the power-law relation

$$P = cA^{-n}$$

where the exponent n depends upon the index chosen but hardly varies from one sample to another. The coefficient c increases with particle size and depends only weakly on whether the particles of a given size are translucent or opaque. The number of available lunar measurements of polarization and albedo on the same feature has not significantly increased since the writing of the Eighth Quarterly Report. But Dr. F. H. Wright, who made extensive visual polarization measurements of many lunar features (F. E. Wright, et al., 1963), will shortly make his data available to us.

#### D. CONCLUSIONS

After analysis of the data on the light-scattering properties of the lunar surface in comparison to those of powder samples bombarded by ions of a simulated solar wind, we conclude that the lunar surface consists of a powder having a very rough macrostructure on a scale of millimeters or more and having particles mostly less than 0.1 mm in size. The particles

probably cannot be translucent or have large, strongly reflecting facets. Neither any accurately measured property of the lunar photometric function nor the polarization of earthlight scattered from the moon permits any conclusion whether the particles are compacted or in an underdense microstructure. It is uncertain whether the opposition effect (abrupt brightness change for phase angles  $|\alpha| < 5^\circ$ ) or the phase angle of maximum polarization will imply an underdense microstructure. The global uniformity of lunar color may arise from the transport of surface atoms caused by sputtering by the solar wind followed by ballistic flight of the atoms to great distance on the moon. The distribution of lunar colors and albedos is in good agreement with the bombarded powder of a chondritic meteorite but the moon is less red than bombarded samples of terrestrial rock powders. Polarization of light scattered from the finely divided, bombarded meteorite is also in good agreement with lunar values but these findings must not be used to infer a lunar surface composition without confirmatory experiments in ultrahigh-vacuum conditions nor without taking into account the global mixing process mentioned above.

A summary of other conclusions from our studies of effects that might be expected from a solar-wind bombardment of the moon was given in the Ninth Quarterly Report: erosion, preferential erosion of some elements, possible powder cementation, etc. Mentioned there and earlier (Wehner et al., 1963b) is the alignment of structures in the ion-bombarded powder surface. This alignment has now been explained as due to large electric forces in the plasma sheath above the sample. Such forces would be far

smaller on the moon, though they are not expected to vanish. Surface electric fields at the moon would probably significantly affect the trajectories of those ions that are formed by sputtering; the fraction of the sputtered flux that is ionic when hydrogen and helium ions of kiloelectron volt energies bombard dielectric solids is unknown.

# REFERENCES

- Anderson, G. S., W. N. Mayer, and G. K. Wehner, Sputtering of dielectrics by high-frequency fields, J. Appl. Phys., 33 (10), 2991-2992, 1962.
- Dollfus, A., Study of the planets by means of the polarization of their light, thesis, University of Paris, 1955; NASA Technical Translation F-188.
- Dollfus, A., Polarization studies of planets, in The Solar System, Vol. 3, Planets and Satellites, pp. 343-399, University of Chicago Press, Chicago, 1961.
- Fessenkov, V. G., Photometry of the moon, in Physics and Astronomy of the Moon, edited by Z. Kopal, pp. 99-130, Academic Press, New York, 1961.
- Gehrels, T., T. Coffeen, and D. Owings, Wavelength dependence of polarization. 3. The lunar surface, Astron. J., 69 (10), 826-852, 1964.
- Green, J., Selection of rock standards for lunar research, Ann. N.Y. Acad. Sci., 123, 1123-1147, 1965.
- Hapke, B., A theoretical photometric function for the lunar surface, J. Geophys. Res., 68 (15), 4571-4586, 1963.
- Hapke, B., Effects of a simulated solar wind on the photometric properties of rocks and powders, Ann. N.Y. Acad. Sci., 123, 711-721, 1965a.
- Hapke, B., Optical properties of the moon's surface, paper presented at the Conference on the Nature of the Surface of the Moon, Goddard Space Flight Center, Greenbelt, Md., April, 1965b.
- Hapke, B., and H. Van Horn, Photometric studies of complex surfaces, with applications to the moon, J. Geophys. Res., 68 (15), 4545-4570, 1963.
- Harris, D. L., Photometry and colorimetry of planets and satellites, in The Solar System, Vol. 3, Planets and Satellites, edited by G. P. Kuiper and B. M. Middlehurst, pp. 272-342, University of Chicago Press, Chicago, 1961.
- Hopfield, J. J., Mechanism of lunar polarization, Science, 151 (3716), 1380-1381, 1966.
- KenKnight, C. E., and G. K. Wehner, Sputtering of metals by hydrogen ions, J. Appl. Phys. 35 (2), 322-326, 1964.
- Kozlova, K. I., and Yu. V. Glagolevskii, Color excesses in six lunar craters according to electrophotometric observations, Astron. Tsirk., No. 198, 1-2, 1958. Redstone Scientific Information Center Translation RSIC-313, Redstone Arsenal, Alabama. AD 608,538.
- Lyot, B., Research on the polarization of light from planets and from some terrestrial substances, Ann. Observ. Paris, Meudon, 8 (1), 1929, NASA Technical Translation F-187.

Minnaert, M., Photometry of the moon, in The Solar System, Vol. 3, Planets and Satellites, edited by G. P. Kuiper and B. M. Middlehurst, pp. 213-248, University of Chicago Press, Chicago, 1961.

Petrova, N. N., Spectral investigations of the lunar surface, *Astron. Zh.*, 43, 162-171, 1966; *Soviet Astron. AJ Engl. Trans.*, 9 (6), 1966.

Rackham, T. W., Photographic colorimetry of the moon in narrow passbands, *Icarus*, 3, 45-51, 1964.

Rosenberg, D. L., and G. K. Wehner, Darkening of powdered basalt by simulated solar-wind bombardment, *J. Geophys. Res.*, 69 (15), 3307-3308, 1964.

Rougier, G., Total photoelectric photometry of the moon, *Ann. Observ. Strasbourg*, 2 (3), 205-239, 1933.

Singer, S. F., and E. H. Walker, Photoelectric screening of bodies in inter-planetary space, *Icarus*, 1, 7-12, 1962.

Smoluchowski, R., Structure and coherency of the lunar dust layer, *J. Geophys. Res.* 71 (6), 1569-1574, 1966.

Stuart, R. V., and G. K. Wehner, Sputtering yields at very low bombarding ion energies, *J. Appl. Phys.*, 33 (7), 2345-2352, 1962.

van den Bergh, S., The color of the moon, *Astron. J.*, 67 (2), 147-150, 1962.

Van Diggelen, J., Photometric properties of lunar crater floors, *Rech. Astron. Observ.*, Utrecht, 14 (2), 1-114, 1958.

Van Diggelen, J., The radiance of lunar objects near opposition, *Planetary Space Sci.*, 13 (4), 271-279, 1965.

Wehner, G. K., Sputtering effects on the moon's surface, *ARS J.*, 31 (3), 438-439, 1961.

Wehner, G. K., C. KenKnight, and D. L. Rosenberg, Sputtering rates under solar-wind bombardment, *Planetary Space Sci.*, 11 (8), 885-895, 1963a.

Wehner, G. K., C. KenKnight, and D. L. Rosenberg, Modification of the lunar surface by the solar-wind bombardment, *Planetary Space Sci.*, 11 (12), 1257-1261, 1963b.

Wilson, O. C., Stellar chromospheres, *Science*, 151 (3717), 1487-1498, 1966.

Wright, F. E., Polarization of light reflected from rough surfaces with special reference to light reflected from the moon, Proc. Natl. Acad. Sci., U.S., 13, 535-540, 1927.

Wright, F. E., F. H. Wright, and H. Wright, The lunar surface: introduction, in The Solar System, Vol. 4, The Moon, Meteorites, and Comets, edited by G. P. Kuiper and B. M. Middlehurst, pp. 1-56, University of Chicago Press, Chicago, 1963.